ISSN: 2538-2152; ECOPERSIA 2023;11(1):47-64.

Improving Rainfall Maps using Precipitation Products of IMERG V06 Final Satellite and Interpolation Methods

ARTICLEINFO

Article Type
Original Research

Author
Morteza Gheysouri, *Ph.D.*[1]
Shahram Khalighi Sigaroodi, *Ph.D.*[2*]
Ali Salajegheh, *Ph.D.*[3]
Bahram Choubin, *Ph.D.*[4]

How to cite this article
Gheysouri M., Khalighi Sigaroodi Sh., Salajegheh A., Choubin B. Improve Rainfall Maps using Precipitation Products of IMERG V06 Final Satellite and Interpolation Methods. ECOPERSIA 2023;11(1): 47-64

DOR:
20.1001.1.23222700.2023.11.1.5.5

[1] Ph.D. Student, Watershed Management, Faculty of Natural Resources Engineering, University of Tehran, Iran.
[2] Associate Professor, Department of Watershed Management Engineering, Faculty of Natural Resources, University of Tehran, Iran.
[3] Professor, Department of Watershed Management Engineering, Faculty of Natural Resources, University of Tehran, Iran.
[4] Soil Conservation and Watershed Management Research Department, West Azarbaijan, Iran

**** Correspondence***
Address: Department of Watershed Management Engineering, Faculty of Natural Resources, University of Tehran, Iran.
Cellphone: (+ 98) 09122727752
Tel: (+98) 02632249313
Fax: (+98) 02632249313
Email: khalighi@ut.ac.ir

Article History
Received: December 2, 2022
Accepted: January 15, 2023
Published: February 15, 2023

ABSTRACT

Aims: This study aims to improve precipitation maps and generalize precipitation to areas without stations.

Materials & Methods: In this study, to improve precipitation maps and increase the accuracy of precipitation maps, linear, multiple regressions and kriging subsets were used. The data from 14 meteorological stations and IMERG images in 20 years (2001 to 2020), a digital elevation model, and latitude and longitude maps of the Kermanshah watershed were used. At first, based on regression in Minitab software, the relationship between air and terrestrial variables was taken. Finally, with the interpolation methods and based on the error coefficients, the best equation for predicting precipitation was determined, and the spatial distribution of precipitation was obtained.

Findings: According to the results, six out of 13 models were selected because of low RMSE and high R^2, R, and NS. Forecast accuracy was reduced in regression models where only one climatic or edaphic variable was used. However, in the models used in the regression elevation, longitude, latitude, and IMERG variables in combination with interpolation methods, the extracted data matched the actual data with a slight difference. In this study, instead of the average of the input variables, the maps of each variable were used, increasing the forecast model's accuracy to R^2=0.8.

Conclusion: The results showed that combining satellite precipitation products with interpolation methods led to a more accurate estimate of precipitation in the points without recording data will be precipitated and the multiple regression method will be more accurate than the linear gradient.

Keywords: *Co-kriging regression, Interpolation, Kermanshah Watershed, Kriging, Precipitation Improvement, Regression. .*

CITATION LINKS

[1] Markonis Y., Papalexiou ... [2] Du Y., Xie Z.Q., ... [3] Breugem A.J., Wesseling J.G., ... [4] Zhong R., Chen X., ... [5] Brodeur Z. P. Steinschneider S. ... [6] Tesfa T.K., Leung L.R. Ghan S.... [7] Zhang L., Ren D., Nan Z., ... [8] Xie P. Xiong A.Y. A ... [9] Golding B.W. ... [10] Gourley J.J. Vieux BE A method for identifying sources of model uncertainty in rainfall-runoff simulations. J. Hydrol. 2006; 327(1-2): 68-80. ... [11] Sorooshian S., ... [12] Zhao H.G., Yang S.T., ... [13] Ghaderpour E., ... [14] Sharifi E., Saghafian B., ... [15] Beck H.E., Wood E.F., Pan M., Fisher C.K., Miralles DG, van Dijk AIJM, McVicar T.R., Adler R.F. MSWEP V2 global 3-hourly 0.1 ◦ precipitation: methodology and quantitative assessment. Bull. Am. Meteorol. Soc. 2019; 100(3): 473–500. ... [16] Baez-Villanueva O.M., ... [17] Hosseini Moghari S.M., Iraqinejad S.H., ... [18] Chen F., Gao Y. Evaluation ... [19] Gupta V., Jain M.K., ... [20] Prakash S., Srinivasan J. ... [21] Hartke S. H., ... [22] Shen Z., Yong B., Yi L., Wu H., Xu H. ... [23] Bharti V., Singh C. ... [24] Ebrahimi S., Chen C., Chen Q., ... [25] Xu R., Tian F., Yang L., Hu H., Lu H., Hou A. ... [26] Nie S., Luo Y., Wu T., Shi X., Wang Z. . ... [27] Yang Z., Hsu K., Sorooshian S., Xu X., Braithwaite D., Zhang Y., Verbist K.M.J. Merging high-resolution satellite-based precipitation fields and point-scale rain gauge measurements-A case study in Chile. J. Geophys. Res. Atmos. 2017; 122(10): 5267–5284. ... [28] Baez-Villanueva-test O.M., ... [29] Xu L., Chen N., Moradkhani H., Zhang X., Hu C. Improving global monthly and daily ... [30] Shen Y., Xiong A., ... [31] Mastrantonas N., Bhattacharya B., ... [32] Zhang X., Tang Q. ... [33] Duan Z., Bastiaanssen W.G.M. ... [34] Bai X., Wu X., Wang P. ... [35] Li M., Shao Q. An improved ... [36] Chao L., Zhang K., Li Z., ... [37] Ma Y., Hong Y., Chen Y., ... [38] Rahman K.U., Shang S., ... [39] Manz B., Buytaert W., ... [40] Chen F., Gao Y., Wang Y., ... [41] Zhang L., Li X., Cao Y., Nan Z., Wang W., Ge Y., ... [42] Chen S., Xiong L., Ma Q., ... [43] Nadi M., Jamei M., Bazrafshan J., Janat Rostami S. Evaluation of different methods for interpolation of mean monthly and annual precipitation data (Case Study: Khuzestan Province). Phys. Geol. Res. 2012; 44(4): 130-117. ... [44] Worqlul A.W., Yen H., ... [45] Poméon T., Jackisch D., ... [46] Kumari M., Basistha A., ... [47] Arowolo A.O., ... [48] Zohrevandi A. A., ... [49] Shahbazi Kh., ... [50] Zolfaghari H., Sahrai J., ... [51] Ghorbanian A., Mohammadzadeh A., ... [52] Huffman G. J., Bolvin D. T., ... [53] Tan J., Huffman G.J., Bolvin D.T., ... [54] Koster R. D., Liu Q., Reichle R. H., ... [55] Ali G., Sajjad M., ... [56] Zhang G., ... [57] Martínez-González A., ... [58] Oliver M.A., ... [59] Kambhammettu BVNP, ... [60] Govaerts Y. M., ... [61] Milewski A., ... [62] Duan Z., Bastiaanssen W. G. M. ... [63] Darand M., ... [64] Pirmoradian R., ... [65] Haberlandt U. ... [66] Verworn A., Haberlandt U. ... [67] Berndt C., Haberlandt U. ... [68] Zou W.Y., Yin S.Q., ... [69] Wang Z., Zhong R., ... [70] Wang Z., Zhong R., Lai C., ... [71] Alsafadi K., Mohammed S., ... [72] Zandi O., Zahraie B., Nasseri M., Behrangi A. ... [73] Daly C., Slater M.E., Roberti J.A., ... [74] Ranhao S., Baiping Z., ...

Introduction

Precipitation is one of the important components in the hydrological and atmospheric cycle, which is not only main for understanding the balance of the water cycle and climate variability [1, 2] but is used for a wide variety of applications, including; flood forecasting [3], drought monitoring [4], water resource management [5], and hydrological and land system modeling [6,7]. However, it is challenging to estimate high-quality precipitation at appropriate spatial and temporal resolutions [8]. Therefore, investigating the spatial changes of precipitation is one of the main inputs of hydrological models and research issues in climate studies. It is challenging to solve them due to the spatial and temporal variability of precipitation. [9, 10, 11, 12]. The lack of basic data, such as precipitation, is considered a limiting factor for climate change studies in developing countries such as Iran. The short duration of time series or low distribution of data collection stations is an important factor in this field. For this reason, researchers and experts have always sought an alternative or an appropriate supplement to obtain information from terrestrial rain gauge [13]. Rain gauges are a traditional and reliable instrument used to measure precipitation on a point scale and are commonly used as benchmarks for evaluating different precipitation products. However, rainfall amounts have a different distribution in most parts of the world [14, 15]. Continuous estimation of spatial variability in precipitation based solely on observations based on rain gauges is subject to great uncertainty [16]. Several methods estimate the amount of precipitation in places without meteorological and rain gauge stations. Today, global precipitation databases, satellite imagery, and interpolation methods have introduced one of the main and valid improvement options for the lack of data [17]. In the past few decades, the rapid development of remote sensing techniques has provided an unprecedented opportunity to estimate precipitation on a global scale continuously. Satellite-based precipitation products (SPPs) are increasingly becoming publicly available, providing users with a powerful understanding of precipitation characteristics [18, 19, 1]. Furthermore, it offers different precipitation products [20, 21, 22]. Nevertheless, precipitation estimation methods using satellite images are relatively complex and have poor performance due to uncertainties and biases of retrieval algorithms, indirect measurements, and lack of sensors (such as false detections of precipitation by infrared sensors in the presence of cold clouds without precipitation and local pressure storms) [23, 24], these cases raise problems in the field of recording spatial and temporal changes in precipitation and sensor limits in the direct observation of effective variations in precipitation formation. Also, using satellite images, the variables obtained are approximate, which will have an indirect and low ratio with the observed precipitation [25]. Precipitation observations based on rain gauges are very accurate but with limited coverage and uneven distribution. On the other hand, satellite-based precipitation products have continuous and wide coverage but with large errors. Therefore, in recent years, many efforts have been made to integrate SPPs and rain gauge observations to improve the accuracy and spatial coverage of precipitation estimates, some of which can be mentioned [26, 27, 18, 15, 28, 29]. (1) Linear interpolation methods, for example, outlier removal [30], weighted distance inverse [31], average squared error [27]; (2) deviance-based methods or residual-based methods, for example, probability mapping method [32], geographic difference/ratio analysis [33, 34]; (3) kernel smoothing methods [35]; (4) approaches with moderate com-

plexity, for example, geographic weighted regression (GWR) [36]; (5) some other more complex methods such as Bayesian averaging method [37,38] and (6) Kriging -based algorithms [39, 40]. Using the above methods, as well as combining satellite products in different areas, has different functions. For example, Zhang et al. [41] reported that the IMERG product performs better than the SM2RAIN-ASCAT product in sub-humid areas of China. Whereas under the semi-arid area, that was the opposite of the situation. Integrating rain gauge-based observations with multiple satellite-based precipitation products rather than a single SPP results in accurate precipitation estimates [42]. In developing countries, where the number of stations with long-term statistics is often very small, the use of the methods mentioned may be significant. For example, the linear gradient methods based on the linear regression relationship between the main and auxiliary variables between the length, width, and elevation of the area, or the three-dimensional linear gradient method by fitting the multiple linear regression multiple regression relationship between the main and auxiliary variables, it can estimate the value of the main variable for the user in unknown points by specifying its latitude, longitude, and elevation [43]. Numerous studies have been carried out to estimate precipitation and study atmospheric precipitation. In this regard, Worqlul et al. [44] evaluated terrestrial precipitation data (CSFR) and (TMPA 3B42) as input data for hydrologic models in sparse data areas. The results showed that TMPA 3B42 cannot describe the temporal changes of rain and that both types of rain gauge data and CFSR reanalysis data can produce river flow data. Poméon et al. [45] as part of a research study, evaluated remote sensing and reanalysis data from the west African region and compared them with existing rain gauge data. The results indicate that satellites with infrared and microwave input data provide better results. Kumari et al. [46] used weighted inverse and kriging family methods to measure precipitation in the Himalayan Mountains. The results showed that the simple kriging method is more efficient for estimating annual precipitation than seasonal precipitation. Arowolo et al. [47] used pattern correction and spline methods to estimate monthly temperature and precipitation in Nigeria. Based on the findings, the spline family methods are more appropriate than the trend correction method. The above shows no meteorological stations in many parts of Iran and the study areas. Therefore, methods should be used to achieve precipitation at any point as pixels to improve precipitation maps. Therefore, the purpose of the upcoming study is to use intermediate methods and multiple regression to establish a relationship between terrestrial and atmospheric variables. Then extracted, pixel point precipitation for the study area. In future research, by combining the above maps with effective environmental variables, it will be possible to achieve precipitation with high accuracy and close to the terrestrial station for areas without meteorological stations.

Materials & methods

Study area

The study was conducted in Kermanshah Province, with an area of 43424 km^2 (i.e., 1.5% of the whole country) located in western Iran, one of the 31 provinces of Iran consisting of 14 townships. The province's capital is Kermanshah. The average annual precipitation in different regions varies from about 300 mm in the southwestern part of Somar and Naftshahr to about 800 mm in the highlands [48]. The average elevation of the province is 1200 m above the average sea level [49]. This province is exposed to

the wet fronts of the Mediterranean, which in the case of dealing with the Zagros highlands, causes rain and snow. Kermanshah Province has two main hot (summer) and cold (winter) seasons. The transitional seasons of spring and autumn are very short and fleeting [50]. According to the important units of Iranian geologic formations, two critical formation zones, namely Zagros and Sanandaj-Sirjan, constitute the general geological structure of Kermanshah Province. The map and location of Kermanshah Province are illustrated in Figure 1.

In the current research, the data of 14 synoptic stations of the Meteorological Organization and rain gauging were used to improve satellite precipitation in areas without stations in Kermanshah province. In addition, 20 monthly satellite images and one annual image of the IMERG V06 Final satellite from 2001 to 2020 were considered. The stations used are shown in Table 1, and their distribution map can also be seen in Figure 1. Due to the complexity of the topography of Kermanshah province and the particular climatic conditions, and the small number of rain gauge stations with long-term periods, especially in the highlands of the province, it becomes difficult to estimate the province's precipitation through interpolation methods, satellite images, and remote sensing. To this end, finding appropriate methods to expand the province's precipitation system can significantly improve statistical quality and error in areas without precipitation stations.

Datasets

In order to achieve an approach to extracting the precipitation map, IMERG Final V06 satellite and station precipitation data were used. Preparing the precipitation map is based on four methods: linear regression, multiple regression, and interpolating loading and coking. This study's precipitation time series was considered for 20 years (2001-2020).

Synoptic Stations

To examine station data performance, data

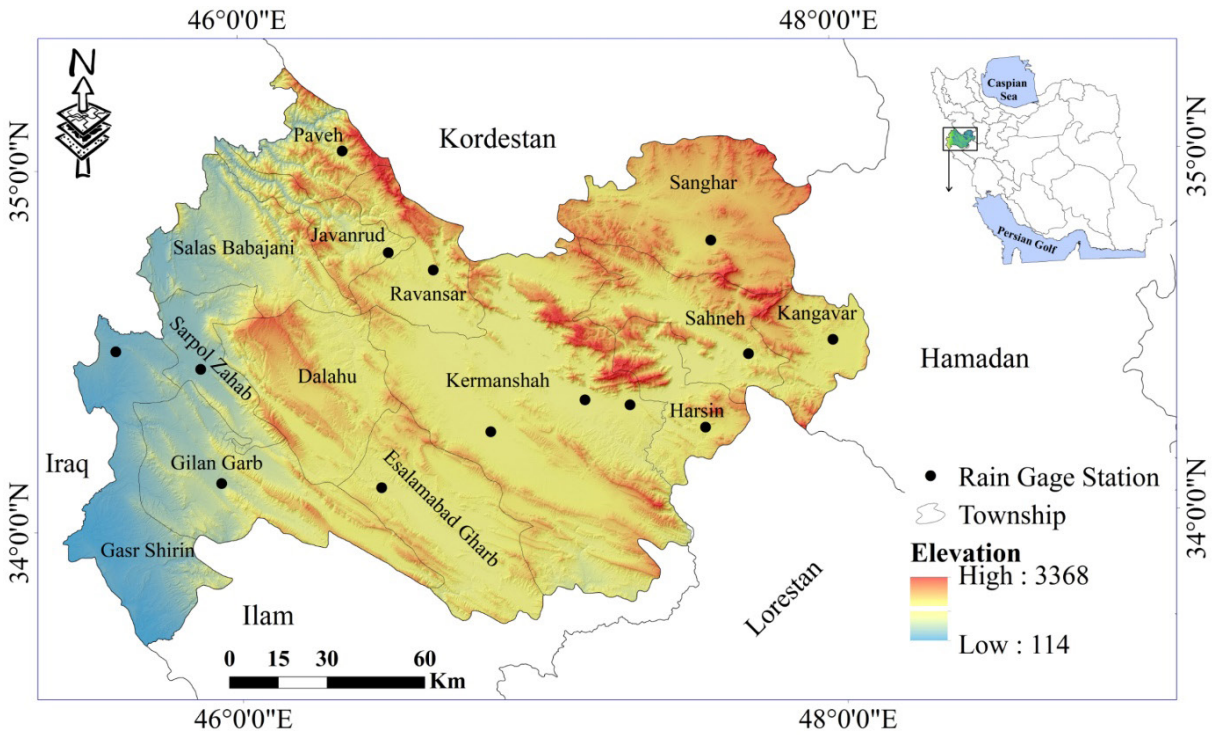

Figure 1) General view of locality and corresponding townships of Kermanshah Province, Iran.

from meteorological stations in Kermanshah province were used for 20 years from 2001 to 2020 (Figure 2). These data were obtained from the Meteorological Organization. Figure 1 shows the distribution of stations within the survey area. In addition, data from the stations were used to prepare linear and multiple precipitation gradients and for validation. The study area has 14 meteorological stations with high spatial distribution, increasing the interpolation maps' accuracy.

Due to the randomness of precipitation data and evaluation criteria based on monthly and annual data, annual and monthly data from terrestrial and air stations were used to increase the accuracy of output results [51].

Integrated Multi-Satellite Retrieval for GPM (IMERG)

This is an international project among satellites from different countries to extract precipitation from 10 precipitation estimation satellites, and the final product is called IMERG. PPS started to implement IMERG algorithm version 6 in the spring of 2019. IMERG6 is the first release available for the TRMM and GPM periods from June 2001. Versions 5, 4, and 3 of the IMERG were issued in late 2017, early 2017, and late 2016, respectively, and are only available for military occupation (April 2014 and later). NASA IMERG industry experts indicated that the latest version of IMERG is suitable for research operations because IMERG V06 is

Table 1) Characteristics of meteorological stations in the study area.

No	Station type	station location	Geographical coordinates		Elevation (m)	Average precipitation mm (Average of 20 years)
			Longitude	Latitude		
1	Airport synoptic	Kermanshah	47.15	34.35	1318.5	415.69
2	Main synoptic	Islamabad-e Gharb	46.47	34.12	1349	468.50
3		Sarpol Zahab	45.87	34.45	545	412.63
4		Kangavar	47.98	34.5	1468	406.83
5		Ravansar	46.65	34.72	1380	526.41
6		Qasr-e Shirin	45.6	34.53	376	356.41
7	Additional synoptic	Gilan-e Gharb	45.93	31.13	816	426.92
8		Javanrud	46.5	34.76	1375	560.415
9		Sonqor	47.58	34.78	1700	409.31
10		Harsin	47.55	34.26	1546	439.5
11		Mahidasht	46.48	34.28	1370	416.32
12	Automatically	Paveh	46.33	35.5	1494	820.65
13		Sahneh	47.66	34.48	1350	483.77
14	Agricultural Meteorological Research	Sararud	47.29	34.33	1361.7	451.66

more suitable than other precipitation satellite products [52]. This model has a spatial resolution of 0.1× 0. 1 ° [53]. In its latest version, IMERG V06, this model includes latitude and longitude of 90° north and south and 180° east and west, including a grid with 3600 columns for latitude and 1800 rows for longitude. IMERG is the most popular data model among more than a dozen data models associated with the GPM project and is represented by PPS at NASA [54]. This satellite's data from 2001 to 2020 was used in this study (Figure 2).

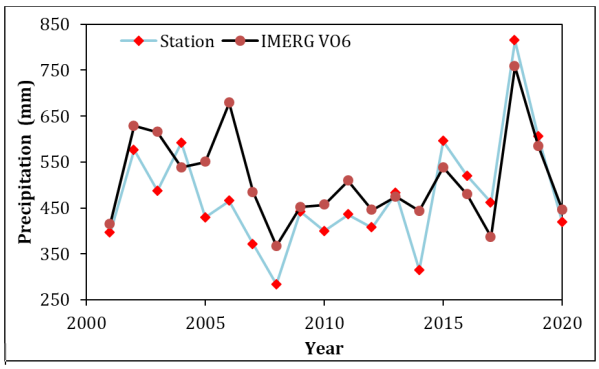

Figure 2). The mean of synoptic stations precipitation observations and IMERG precipitation between 2001 and 2020 were used to validate and intercompare the selected Gridded Precipitation Products (GPPs).

Optimal precipitation interpolation methods

Because elevation changes are one of the primary variables in the creation of precipitation events in a region. Consequently, the choice of an interpolation method that can accurately predict precipitation is variable [55]. This research has analyzed almost four known interpolation methods (linear regression, multiple regression, kriging, and co-kriging). They were then analyzed based on error assessment criteria, and the best method was determined from the available methods.

Linear regression model

In the gradient method, it is assumed that there are different trends in different directions in the study area, and it is assumed that this trend is in the direction of a degree polynomial. In the linear gradient method, and should be identical in different directions. This average shows that the studied spatial variable changes linearity in all directions. The spatial variable under investigation is assumed to change linearly in all directions. The scale of the linear regression approach is the number of independent variables [56]. These independent variables generally include two groups of geographic location variables (latitude and longitude) and topographic variables (elevation, amount, and direction of slope) Eq. (1). In this study, in order to prepare a precipitation map, a linear regression was formed from the relationship between precipitation changes and elevation. Then, a precipitation map was prepared for the study area using a DEM of the study area.

$$P = ax + b \qquad \text{Eq. (1)}$$

where a is the width of the source, b is the gradient, x is the elevation in m, and P is the precipitation of pixels in mm.

Linear multiple regression model

This study used the RML method to create multiple linear relationships for precipitation prediction using elevation data and IMERG. Multiple regression analysis is used when the value of an individual variable can be predicted from the values of other variables. The overall relationship of the RML model for (n) independent variables is presented in Eq. (2).

$$P = \beta_1 X_1 + \beta_2 X_2 + \ldots\ldots + \beta_n X_n + \varepsilon \qquad \text{Eq. (2)}$$

where P represents the dependent variable, X1 to Xn represents the independent variables to represent the regression coefficients, and ε is a random constant. The MiniTab22 software was used in this study

to analyze linear and multiple regression among the studied variables.

Geostatistical analysis (Kriging and Co-Kriging)

Interpolation methods can be divided into deterministic interpolation and geostatistical interpolation [57]. Consequently, in this research, two methods of kriging (normal, single) and co-kriging were used to examine and prepare the distribution map. The basis of this geostatistical assumption [58] is summarized in Eq. (3).

$$P_{(X)} = \mu_{(X)} + \varepsilon_{(X)} \quad \text{Eq. (3)}$$

Where P(x): variability of precipitation, μ(x): (average precipitation), and autocorrelated random variation ε (x) at location x [59, 58].

In addition to regular kriging, co-kriging has also been used. The most common use of co-kriging is when the covariates are more accessible and, therefore, denser (or even more comprehensive) sampled than the target variable. Conventional co-kriging investigates the spatial relations between two or more variables by determining their co-location [60]. This approach, like multivariate regression, allows various variables to be used to assess and improve the spatial precipitation prediction model.

Statistical evaluation - total error

To compare the predicted values with the measured data, several criteria are used, including correlation coefficient (R), coefficient of determination (R^2), root average square error (RMSE), and Nash-Sutcliffe model efficiency coefficient (NSCE). The correlation factor measures the linear correlation between station observations and satellite estimates. The Eq. associated with the criteria mentioned above is explained in Table 2.

Findings

A precipitation map of the province of Kermanshah was developed using two standard interpolations (Figure 3-A) and regression methods (Figure 3-B). The average precipitation for the study area is 469.4 mm using the interpolation method and 490.50 mm using the regression method. These values differ by -1.67 and 19.43 mm from the actual average of the 14 studied stations, i.e., 471.07 mm, for the interpolation and regression methods, respectively. To enhance the precipitation gradient and prepare a precipitation map, 13 regression equations were prepared between precipitation and photographs and atmospheric variables (Table 3). Table (3) presents Precipitation regression

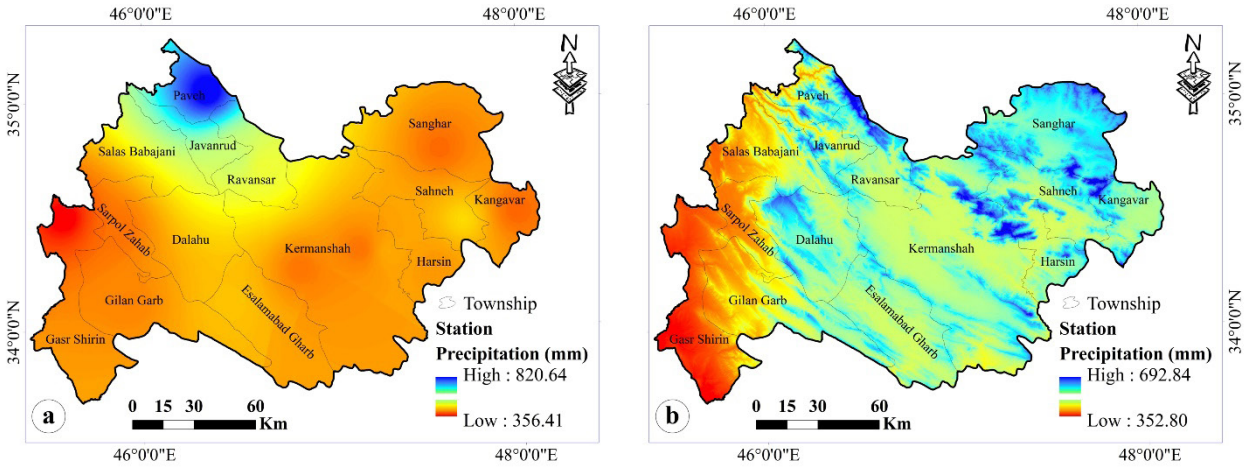

Figure 3) A precipitation map of Kermanshah province based on the interpolation method (a) and gradient method (b).

Table 2) The statistical evaluation indices to evaluate quantitative Rain estimates.

Metrics	Eq.	Eq. No.
Correlation coefficient (R)	$\frac{\sum_i^n (Xi - \bar{X})(Yi - \bar{Y})}{\sqrt{\sum_i^n (Xi - \bar{X})^2}\sqrt{\sum_i^n (Yi - \bar{Y})^2}}$	Eq. (4)
Coefficient of determination (R^2)	R*R	Eq. (5)
RMSE	$\sqrt{\frac{\sum_{t=1}^n (Yi - X_i)^2}{n}}$	Eq. (6)
NSCE	$\frac{\sum_{t=1}^n (X_i - Yi)^2}{\sum_{t=1}^n (X_i - \bar{X}_i)^2}$	Eq. (7)

Note: n is the number of observations in the sample; *Xi* and *Yi* represent the *i*th gauge observation and estimates data, respectively; *X* and *Y* are the corresponding samples' average values

Table 3) Adjustment of the regression equation for the study area.

Input Variable	Regression Eq.	Eq. No.
IMERG VO6 Final	-379 + 1.684 × IM	Eq. (8)
Elevation	382 + 0.0780 × El	Eq. (9)
Longitude	2039 - 33.3 × Lon	Eq. (10)
Latitude	-689 + 34.0 × Lat	Eq. (11)
Longitude, Latitude	1232 - 47.9 × Lon+ 43.4× Lat	Eq. (12)
Longitude , Latitude , IMERG	-459 - 0.8× Lon + 3.8 × Lat + 1.661× IM	Eq. (13)
Longitude, Latitude, IMERG, Elevation	-187 - 6.7 × Lon + 4.0 × Lat + 1.616 × IM + 0.012 × El	Eq. (14)
Longitude, Latitude, Elevation	6611 - 156.5 × Lon + 24.3 × Lat + 0.2903 × El	Eq. (15)
Longitude, Elevation	7474 - 157.8 × Lon + 0.3140 × El	Eq. (16)
Latitude, Elevation	-498 + 26.5 × Lat + 0.0541 × El	Eq. (17)
Latitude, IERG	-491 + 3.5 × Lat + 1.665 × IM	Eq. (18)
Longitude, ERG	-427 + 1.0 × Lon + 1.687 × IM	Eq. (19)
IMERG, Elevation	-380 + 1.677 × IM + 0.0032 × El	Eq. (20)

equations linearly and multivariate.

Then, using the equation extracted for each station, the amount of precipitation was prepared by placing the elevation and the average pixel point of satellite precipitation and soil variables (Table 4). According to Table (4), in the models where the precipitation variable was extracted based on multiple regressions, the precipitation was more accurately predicted for each station. Models 1, 2, 6, 7, 11, and 13 could predict precipitation for the study area with more precision than other predicted models. Model 12 has a high R^2 coefficient but was rejected because of the high ESMN and Nash-Sutcliffe.

One of the primary variables that have made the model more accurate is the variability of precipitation as a function of longitude and latitude (Table 4). In the investigation of changes in precipitation caused by terrestrial variables of longitude and latitude, it was found that the accuracy of the regres-

sion model increases when the latitude is combined with satellite images. On the other hand, longitude, in combination with altitude, predicts precipitation more accurately.

Investigating the spatial changes of precipitation

In order to check the location of fitted precipitation models for the study area, point precipitation was estimated based on regression models in each station. Then a precipitation map was prepared based on kriging and co-kriging models (Figures 4 & 5). In Figure (3), the maximum spatial distribution of precipitation was observed in the northern and central slopes (including Paveh, Javanrud, Dalahu, and Eslamabad-e Gharb) and the least in the western-eastern slopes (including Salas Babajani, Qasr-e Shirin, Hersin, and Kangavar). In this section, the zoned maps were divided into two groups, single and multiple variables. This separation obtains the best possible situation for the spatial interpretation of precipitation based on the type of image received from different regression methods (single-variable and multiple regression).

According to Figure (4), in the spatial distribution of precipitation based on elevation regression (El), the maximum precipitation has moved to the higher parts of the study area, and the minimum precipitation is in the western part. When the satellite station (IMERG V06) was used to prepare perception regression, the created perception map coincided with the station perception map. However, the difference is that the percep-

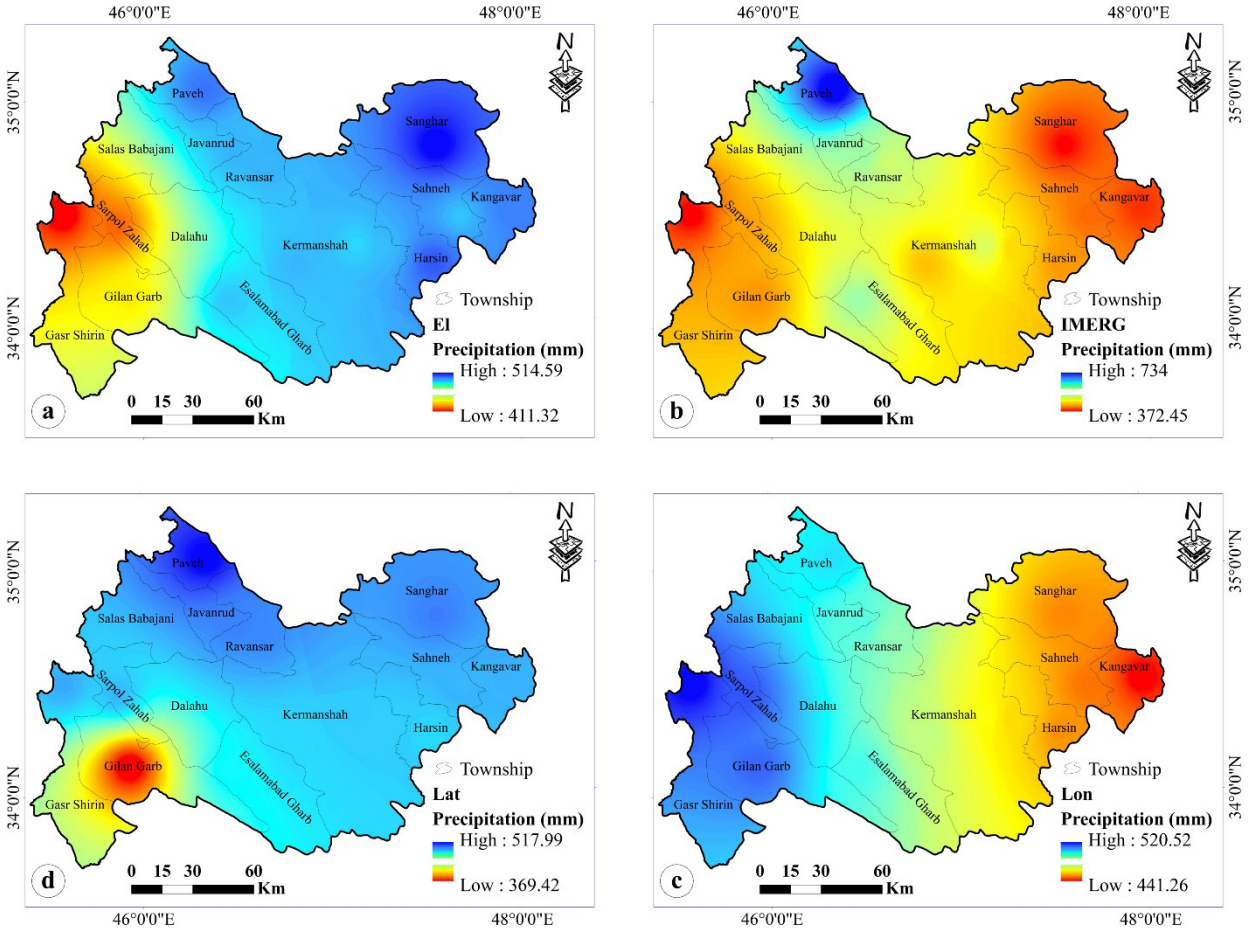

Figure 4) Spatial distribution of precipitation in Kermanshah province based on single-variable regression and Kriging (Elevation (a), IMERG (b), Longitudes (c), Latitude (d)).

Table 4) Adjusted model average error values for the Kermanshah meteorological station.

Eq. No.	Input Variable	RMSE	R (XY)	NS	R^2
Eq. (8)	IMERG VO6 Final	51.45	0.89	0.78	0.78
Eq. (9)	Elevation	103.00	0.35	0.11	0.13
Eq. (10)	Longitude	109.33	0.12	0.00	0.02
Eq. (11)	Latitude	101.69	0.38	0.13	0.15
Eq. (12)	Longitude, Latitude	98.94	0.43	0.18	0.19
Eq. (13)	Longitude, Latitude , IMERG	51.05	0.89	0.78	0.79
Eq. (14)	Longitude, Latitude, IMERG, Elevation	50.36	0.89	0.79	0.79
Eq. (15)	Longitude, Latitude, Elevation	71.81	0.76	0.57	0.58
Eq. (16)	Longitude, Elevation	76.55	0.72	0.51	0.51
Eq. (17)	Latitude, Elevation	98.72	0.45	0.18	0.20
Eq. (18)	Latitude, IMERG	50.56	0.89	0.79	0.79
Eq. (19)	Longitude, IMERG	93.95	0.91	0.26	0.81
Eq. (20)	IMERG, Elevation	51.12	0.89	0.78	0.79

tion obtained from satellite images is less intense in low altitude and plain areas. The influence of longitude and latitude in the study area showed that the longitudes in the Zagros highlands effectively influenced precipitation. The precipitation is higher in the western regions of the province, which have shorter latitudes, and the precipitation decreases as it goes to higher latitudes (east of the region). So Sarpol Zahab has the most perception, and Kangavar shows the least rainfall.

Nevertheless, in longitudes, this characteristic is reversed. High longitudes have more precipitation, and low longitudes have less precipitation. The images prepared for several precipitation-affected soil variables were predicted with higher spatial accuracy than the single variable (Figure 5).

In multiple regression, the spatial distribution of rainfall is more accurate due to the implication of various factors affecting rainfall. According to Figure 5, when two factors with different characteristics such as terrestrial and climate variables (Figure 5, a & b) are used to prepare the precipitation map, precipitation is predicted more accurately. To confirm this result, Figure (5, c & d) consists of two terrestrial latitude and longitude variables with altitude. Precipitation has an inconsistent distribution, so in areas shown for longitude and altitude, it is the opposite of longitude and latitude s. As a result, the spatial precision of precipitation is less than the main precipitation map in Figure (3). The predicted rainfall has an acceptable accuracy due to its multifactorial nature (Figures 5e & f).

In general, the preparation of the precipitation maps was based on the average of the precipitation extracted and the station's height in the form of station points. Consequently, the precipitation zone is only sometimes accurate in areas with no scattered stations. In this regard, the 1km precipitation map of IMERG V06 satellites was converted to a digital pixel size of 27 meters using resample and aggregate commands in ArcGIS

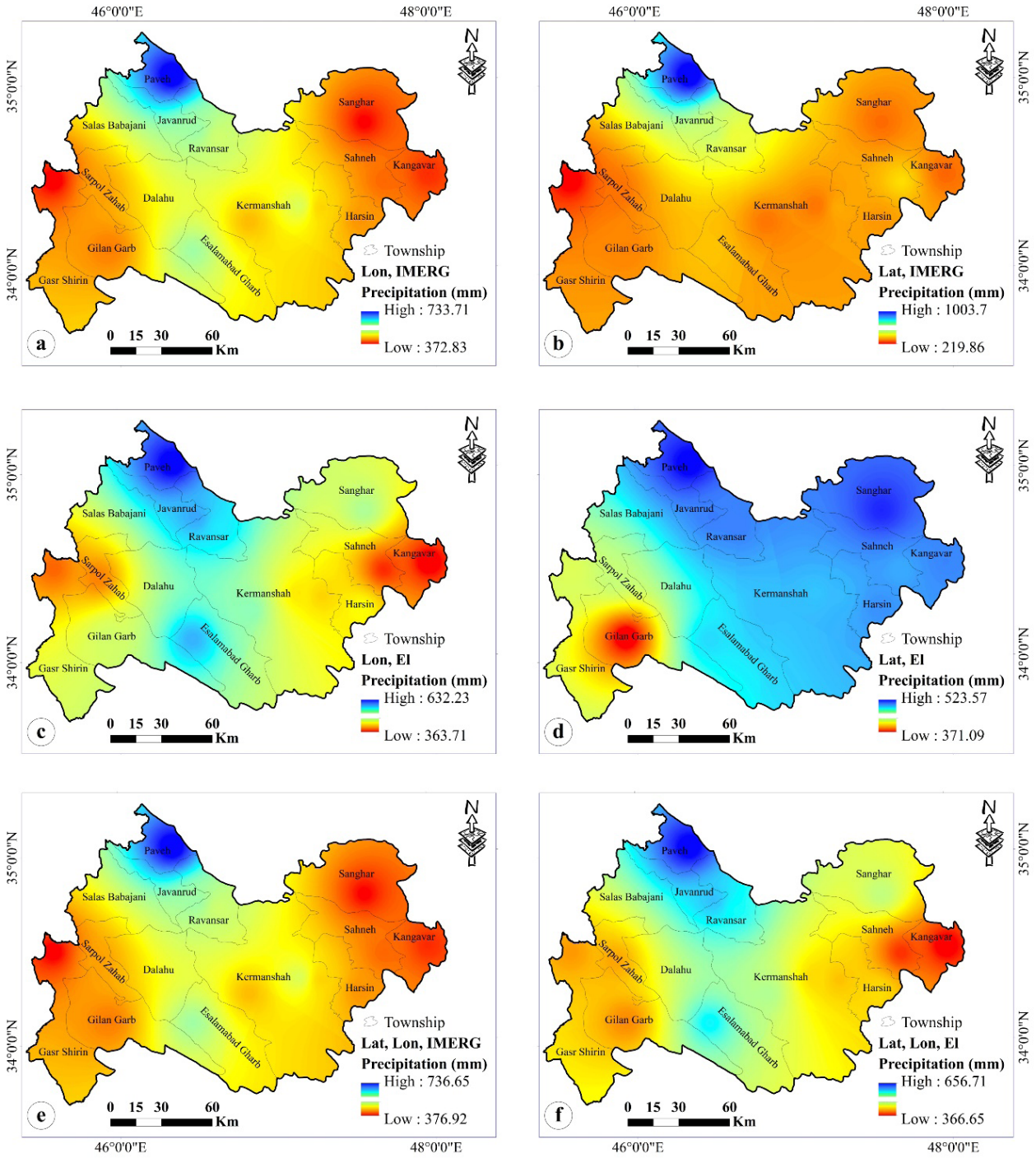

Figure 5) Spatial distribution of precipitation in Kermanshah province based on multiple regression and co-Kriging (Longitudes+ IMERG (a), latitude + IMERG (b), Longitudes+ Elevation (c), Latitude + Elevation (d), Latitude+ Longitudes+IMERG (e), Latitude+ Longitudes+ Elevation (f)).

10.8.1 software. The longitude and latitude maps were also prepared and entered into the multiple regression equation of precipitation. In Figure (6), these maps were prepared in the above station forms and pixel forms for the study area.

Precipitation was extracted by interpolation with the multiple regression method, but the map is extracted from the average station changes and in point form (Figure 6, a1 & b1). The averages for each pixel were obtained by multiplying the maps of each vari-

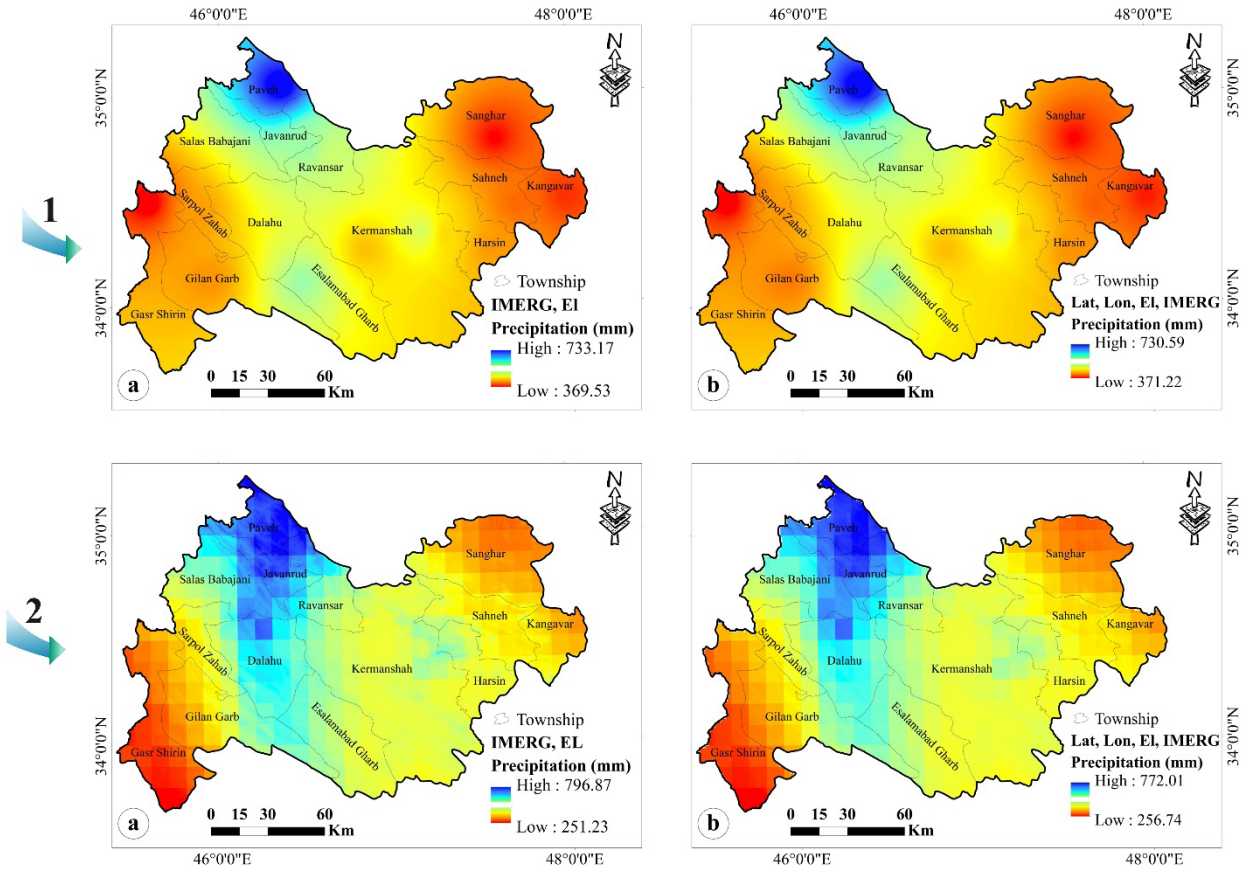

Figure 6) Spatial distribution of precipitation in Kermanshah province in two ways, interpolation and pixel (IMERG + Elevation (a1), Latitude+ Longitudes + Elevation+ IMERG (b1), IMERG + Elevation (a2), Latitude+ Longitudes + Elevation+ IMERG (b)).

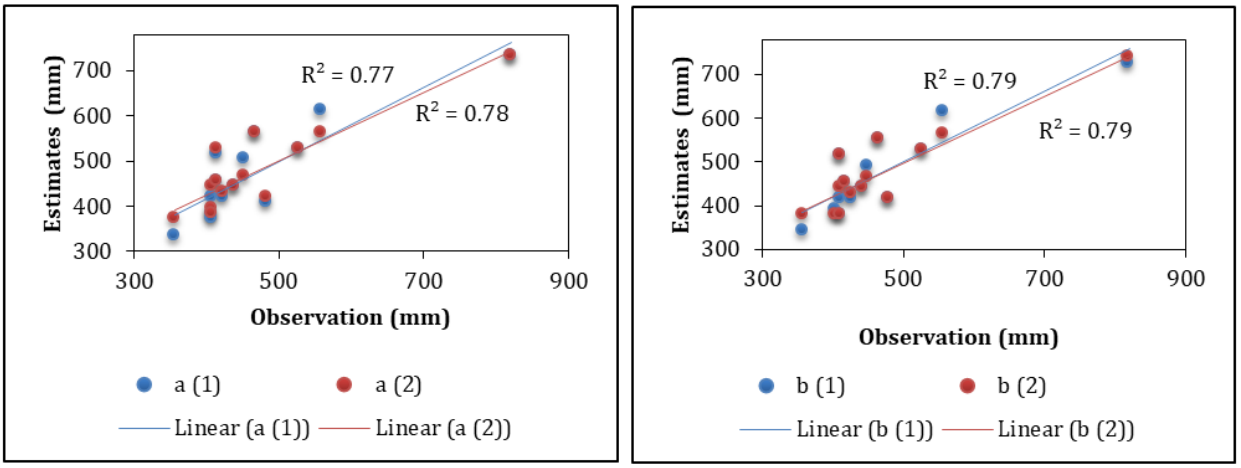

Figure 7) Regression analysis of different methods of locating precipitation data.

able in the adjusted model (Figure 6, a2&b2). Figure 7, the gradient diagram shows the observed and projected precipitation from the regression Eq.

For the regression analysis of the methods used in this research, station interpolation regression and multiple regression were drawn, and their results were almost the same and similar. In order to determine the best-fitted model, the estimated graph and the actual

amount of precipitation were drawn against each other, and the line equation for different interpolation methods was also fitted to the data. According to the equation and the resulting diagram, the best line equation is related to the four-dimensional gradient method, which is the closest line to the 1:1 line compared to other methods. The regression analysis results presented the four dimensions multiple gradient method (Figure 7, b1, and b2) as the superior method.

Discussion

This research was conducted to study the possibility of combining satellite precipitation products and interpolation methods. In addition to verifying the accuracy of the IMERG precipitation network data, the accuracy of the proposed method was also verified using interpolating methods. The precipitation areas of Kermanshah province were extracted with linear and multiple regression. In the single-variable approach, the models provided were not of acceptable accuracy due to the influence of a factor in the precipitation estimate (Table 4). However, they have high accuracy in multivariable models due to the influence of several factors. Considering that in Kermanshah province and the western regions of Iran, precipitation enters the country from the west, it is expected that the precipitation will be a maximum in the western regions.

Nevertheless, the precipitation has concentrated in the region's northern and central parts, so the minimum amount was observed in the Salas Babajani area, and the maximum amount was observed in Paveh (Figure 3). In this situation, there are two influential factors: the inappropriate distribution of meteorology stations due to the mountainous area and the poor performance of IMERG satellite observation in mountainous areas, which has caused errors in precipitation [61, 62, 63, 64]. In examining the spatial changes of precipitation in all the zoned forms with the interpolation method, the maximum precipitation is concentrated in the mountainous and northern regions of the study area. These changes show a better performance of interpolation methods in predicting precipitation in mountain areas (Figures 4&5). The findings of this research are consistent with those of the interpolation studies [65, 66, 67, 68]. By examining the location of precipitation and comparing single and multiple regression interpolation methods, it was found that the precipitation map, combined with terrestrial variables or satellite image data in a two-variable manner, is less accurate in estimating precipitation. For example, in Figure 5, when precipitation or elevation alone or combined with one of the terrestrial variables, such as longitude and latitude, the accuracy of the forecast changed, and the precipitation was far from the actual value. When combined with the terrestrial bivariate variability, the estimated accuracy is lower due to the characteristics of the IMERG gauge for recording precipitation (Figure 6). Thus, it records light and moderate rains well but performs poorly in detecting heavy rains [69, 70]. Therefore, recourse to multiple regression reduces this influence (Figure 6). Because the multiple regression method estimates the dependent variability as a function of correlation and across independent variables, it has obtained more acceptable results for modeling precipitation at higher altitude levels that lack measurement stations, which is in line with the results of the research of Alsafadi et al. [71]. The problem in many meteorological studies is the imposition of precipitation for areas with stations to areas without stations, which causes the user to make an error in predicting precipitation. Therefore, by combining and placing IMERG satellite precipitation maps and elevation, latitude, and longitude in the four-dimensional regression equation, a map was

prepared that had a coefficient of determination of 0.79 %, which is more accurate than the standard method of estimating precipitation. Because in the areas that did not have a station, precipitation was received from satellite images, which increased the accuracy of the map, which agrees with the results of Zandi et al. [72]. The combination of meteorological and advisory data can effectively improve precipitation maps and better-predict precipitation for areas without stations. Therefore, this method has shown high efficiency in improving results, particularly in estimating annual precipitation, as mentioned in several studies [73, 74].

Conclusion

This study was carried out to obtain new perception data with high spatial resolution in areas without stations or with limited stations and also to determine the best approach to integrating statistical methods with spatial interpolation analysis in GIS software. Two standard interpolation methods, kriging and regression, and their subset were used to estimate precipitation. In this study, the use of perception satellite images increases the accuracy of interpolation and regression methods and reduces errors in areas without stations. In order to improve the performance of multiple regression methods, the combination of high-precision IMERG satellite precipitation data obtained from GPM was used, and the summary of the results is as follows:

• Precipitation data obtained from interpolation methods are acceptable in estimating precipitation.

• The multiple regression method combined with the interpolation methods increased the quality of the estimated precipitation in most of the stations studied.

• R^2, and NS coefficients had values close to one for multiple regressions.

• The use of multiple regression (placing the map of influential variables in the model) increased the R^2 coefficient.

The R^2 coefficient is a source of error in precipitation estimation.

• The extracted maps show that IMERG products have a high spatial and temporal resolution to improve and forecast precipitation.

Based on these results, future research should focus on error correction and the application of precipitation correction to climate and hydrological studies in the region. The results of this study may also help developers of precipitation improvement algorithms and the microscale scale of climate settings.

Acknowledgments

The authors sincerely thank the University of Teheran for this research's formal and financial support.

Ethical permissions: The authors of this study approve sending it to ECOPERSIA journal and declare that this study is not under revision in any other scholarly journals at the time of submission to the journal and will not be sent to any other scholarly journal during the revision at the journal until the definite answer about it. The authors chose Dr. Shahram Khalighi Sigaroodi (Second author) as the corresponding author and delegated all the responsibility of the article to her regarding following the relation with ECOPERSIA.

Conflict of Interest: The authors declare that there is no conflict of interest regarding the publication of this study.

Authors' Contribution: Morteza Gheysouri (First author), Introduction author/Methodologist/
Original researcher/Discussion author (25%); Shahram Khalighi Sigaroodi (Second author), Introduction author/ Methodologist/ Discussion author (25%); Ali Salajegheh (Third author), Introduction/data analysis and writing Methodologist (25%);

Bahram Choubin (Third author), Introduction/data analysis and writing Methodologist (25%).

Funding/Support: The University of Tehran of Iran supported the present study.

References

1. Markonis Y., Papalexiou S.M., Martinkova M., Hanel M. Assessment of water cycle intensification over land using a multisource global gridded precipitation dataset. J. Geophys. Res. Atmos. 2019; 124(21):11175-11187.
2. Du Y., Xie Z.Q., Miao Q. Spatial scales of heavy meiyu precipitation events in eastern china and associated atmospheric processes. Geophys. Res. Lett. 2020; 47(11):1-9.
3. Breugem A.J., Wesseling J.G., Oostindie K., Ritsema, C.J. Meteorological aspects of heavy precipitation in relation to floods–an overview. Earth-Sci. Rev.103171 :204 ;2020 .
4. Zhong R., Chen X., Lai C., Wang Z., Lian Y., Yu H., Wu, X. Drought monitoring utility of satellite-based precipitation products across mainland China. J. Hydrol. 2019; 568(1):343–359.
5. Brodeur Z. P. Steinschneider S. Spatial bias in medium-range forecasts of heavy precipitation in the Sacramento river basin: implications for water management. J. Hydrometeorol.2020; 21(7):1405-1423.
6. Tesfa T.K., Leung L.R. Ghan S.J. Exploring topography-based methods for downscaling subgrid precipitation for use in Earth System Models. J . Geophys. Res. Atmos. 2020; 125(5):1-24.
7. Zhang L., Ren D., Nan Z., Wang W., Zhao Y., Zhao Y., Ma Q., Wu X. Interpolated or satellite-based precipitation? Implications for hydrological modeling in a meso-scale mountainous watershed on the Qinghai-Tibet Plateau. J. Hydrol.2020; 583(1):1-15.
8. Xie P., Xiong A.Y. A conceptual model for constructing high-resolution gauge-satellite merged precipitation analyses. J. Geophys. Res. Atmos. 2011; 116(D21).
9. Golding B.W. Uncertainty propagation in a London flood simulation. J. Flood Risk Manag. 2009; 2(1):2-15.
10. Gourley J.J., Vieux B.E. A method for identifying sources of model uncertainty in rainfall-runoff simulations. J. Hydrol. 2006; 327(1-2):68-80.
11. Sorooshian S., AghaKouchak A., Arkin P., Eylander J., Foufoula-Georgiou E., Harmon R., Hendrickx J.M., Imam B., Kuligowski R., Skahill B., Skofronick-Jackson G. Advanced concepts on remote sensing of precipitation at multiple scales. Bull. Am. Meteorol. Soc. 2011; 92(10):1353-1357.
12. Zhao H.G., Yang S.T., Wang Z.W., Zhou X., Luo Y., Wu L.N. Evaluating the suitability of TRMM satellite rainfall data for hydrological simulation using a distributed 42 hydrological model in the Weihe River catchment in China. J. Geogr. Sci. 2015; 25(2):177-195.
13. Ghaderpour E., Ben Abbes A., Rhif M., Pagiatakis S.D., Farah, I. R. Non-stationary and unequally spaced NDVI time series analyses by the LSWAVE software. Int. J. Remote Sens. 2020; 41(6):2374-2390.
14. Sharifi E., Saghafian B., Steinacker R. Downscaling satellite precipitation estimates with multiple linear regression, artificial neural networks, and spline interpolation techniques. J. Geophys. Res. Atmos. 2019; 124(2):789–805.
15. Beck H.E., Wood E.F., Pan M., Fisher C.K., Miralles DG, van Dijk AIJM, McVicar T.R., Adler R.F. MSWEP V2 global 3-hourly 0.1° precipitation: methodology and quantitative assessment. Bull. Am. Meteorol. Soc. 2019; 100(3):473–500.
16. Baez-Villanueva O.M., Zambrano-Bigiarini M., Beck H.E., McNamara I., Ribbe L., Nauditt A., Birkel C., Verbist K., Giraldo-Osorio J.D., Xuan Thinh N. RFMEP: A novel Random Forest method for merging gridded precipitation products and ground-based measurements. Remote Sens. Environ. 2020; 239:111606: 196-201.
17. Hosseini Moghari S.M., Iraqinejad S.H., Ebrahimi K. Evaluation of global rainfall bases and their application in drought monitoring-Case (Karkheh basin). J. Agric. Meteorol. 2016; 102(2) :14-26.
18. Chen F., Gao Y. Evaluation of precipitation trends from high-resolution satellite precipitation products over Mainland China.Clim.Dyn. 2018;51(9–10):3311–3331.
19. Gupta V., Jain M.K., Singh P.K., Singh V. An assessment of global satellite-based precipitation datasets in capturing precipitation extremes: A comparison with observed precipitation dataset in India. Int. J. Climatol. 2019; 40(8):3667–3688.
20. Prakash S., Srinivasan J. A comprehensive evaluation of near-real-time and research products of imerg precipitation over India for the southwest monsoon period. Remote Sens. 2021; :(18)13 1-19.
21. Hartke S. H., Wright D. B. Where Can IMERG Provide a Better Precipitation Estimate than Interpolated Gauge Data? Remote Sens. 2022; 14(21): 1-19.
22. Shen Z., Yong B., Yi L., Wu H., Xu H. From TRMM to GPM, how do improvements of post/near-real-time satellite precipitation estimates manifest? Atmos. Res. 2022; 268(1): 106029.
23. Bharti V., Singh C. Evaluation of error in TRMM 3B42V7 precipitation estimates over the Himalayan region. J. Geophys. Res. Atmos. 2015;

120(24): 12458–12473.
24. Ebrahimi S., Chen C., Chen Q., Zhang Y., Ma N., Zaman Q. Effects of temporal scales and space mismatches on the TRMM 3B42 v7 precipitation product in a remote mountainous area. Hydrol. Process. 2017; 31(24): 4315–4327.
25. Xu R., Tian F., Yang L., Hu H., Lu H., Hou A. Ground validation of GPM IMERG and TRMM 3B42V7 rainfall products over southern Tibetan Plateau based on a high-density rain gauge network. J. Geophys. Res. Atmos. 2017; 122(2): 910–924.
26. Nie S., Luo Y., Wu T., Shi X., Wang Z. A merging scheme for constructing daily precipitation analyses based on objective bias-correction and error estimation techniques. J. Geophys. Res.: Atmos. 2015; 120 (17): 8671–8692.
27. Yang Z., Hsu K., Sorooshian S., Xu X., Braithwaite D., Zhang Y., Verbist K.M.J. Merging high-resolution satellite-based precipitation fields and point-scale rain gauge measurements-A case study in Chile. J. Geophys. Res. Atmos. 2017; 122(10): 5267–5284.
28. Baez-Villanueva-test O.M., Zambrano-Bigiarini M., Beck H.E., McNamara I., Ribbe L., Nauditt A., Birkel C., Verbist K., Giraldo-Osorio J.D., Xuan Thinh N. RFMEP: A novel random forest method for merging gridded precipitation products and ground-based measurements. Remote Sens. Environ. 2020; 239: 111606.
29. Xu L., Chen N., Moradkhani H., Zhang X., Hu C. Improving global monthly and daily precipitation estimation by fusing gauge observations, remote sensing, and reanalysis datasets. Water Resour. Res. 2020; 56(3): e2019WR026444.
30. Shen Y., Xiong A., Hong Y., Yu J., Pan Y., Chen Z., Saharia M. Uncertainty analysis of five satellite-based precipitation products and evaluation of three optimally merged multi-algorithm products over the Tibetan Plateau. Int. J. Remote Sens. 2014; 35(19): 6843.
31. Mastrantonas N., Bhattacharya B., Shibuo Y., Rasmy M., Espinoza-D'avalos G., Solomatine D. Evaluating the benefits of merging near-real-time satellite precipitation products: a case study in the Kinu Basin Region, Japan. J. Hydrometeorol. 2019; 20(6): 1213–1233.
32. Zhang X., Tang Q. Combining satellite precipitation and long-term ground observations for hydrological monitoring in China. J. Geophys. Res.: Atmos. 2015; 120(13): 6426–6443.
33. Duan Z., Bastiaanssen W.G.M. First results from Version 7 TRMM 3B43 precipitation product in combination with a new downscaling–calibration procedure. Remote Sens. Environ. 2013; 131(1): 1–13.
34. Bai X., Wu X., Wang P. Blending long-term satellite-based precipitation data with gauge observations for drought monitoring: Considering effects of different gauge densities. J. Hydrol. 2019; 577: 124007.
35. Li M., Shao Q. An improved statistical approach to merge satellite rainfall estimates and rain gauge data. J. Hydrol. 2010; 385 (1–4): 51–64.
36. Chao L., Zhang K., Li Z., Zhu Y., Wang J., Yu Z. Geographically weighted regression-based methods for merging satellite and gauge precipitation. J. Hydrol. 2018;558(1):275–289.
37. Ma Y., Hong Y., Chen Y., Yang Y., Tang G., Yao Y., Long D., Li C., Han Z., Liu R. Performance of optimally merged multi-satellite precipitation products using the dynamic bayesian model averaging scheme over the Tibetan Plateau. J. Geophys. Res. Atmos. 2018;123(2): 814–834.
38. Rahman K.U., Shang S., Shahid M., Wen Y., Khan Z. Application of a dynamic clustered bayesian model averaging (DCBA) algorithm for merging multi-satellite precipitation products over Pakistan. J. Hydrometeorol. 2020; 21(1): 17–37.
39. Manz B., Buytaert W., Zulkafli Z., Lavado W., Willems B., Robles L.A., Rodríguez- S´anchez J.-P. High-resolution satellite-gauge merged precipitation climatologies of the Tropical Andes. J. Geophys. Res. Atmos. 2016; 121(3): 1190–1207.
40. Chen F., Gao Y., Wang Y., Li X. A downscaling-merging method for high-resolution daily precipitation estimation. J. Hydrol. 2020a; 581: 124414.
41. Zhang L., Li X., Cao Y., Nan Z., Wang W., Ge Y., Wang P., Yu W. Evaluation and integration of the top-down and bottom-up satellite precipitation products over mainland China. J. Hydrol. 2020a; 581: 124456.
42. Chen S., Xiong L., Ma Q., Kim J.-S., Chen J., Xu C. Y. Improving daily spatial precipitation estimates by merging gauge observation with multiple satellite-based precipitation products based on the geographically weighted ridge regression method. J. Hydrol. 2020b; 589: 125156.
43. Nadi M., Jamei M., Bazrafshan J., Janat Rostami S. Evaluation of different methods for interpolation of mean monthly and annual precipitation data (Case Study: Khuzestan Province). Phys. Geol. Res. 2012; 44(4): 130-117.
44. Worqlul A.W., Yen H., Collick A.S., Tilahun S.A., Langan S., Steenhuis TS Evaluation of CFSR, TMPA 3B42 and ground-based rainfall data as input for hydrological models, in data-scarce regions: The upper Blue Nile Basin, Ethiopia. Catena. 2017; 152(1): 242-251.
45. Poméon T., Jackisch D., Diekkrüger B. Evaluating the performance of remotely sensed and reanalysed precipitation data over West Africa using HBV light. J. Hydrol. 2017; 547(1):222-235.
46. Kumari M., Basistha A., Bakimchandra O., Singh C.K. Comparison of spatial interpolation meth-

ods for mapping rainfall in Indian Himalayas of Uttarakhand region. In geostatistical and geospatial approaches for the characterization of natural resources in the environment 2016; 159-168.
47. Arowolo A.O., Bhowmik A.K., Qi W., Deng X. Comparison of spatial interpolation techniques to generate high-resolution climate surfaces for Nigeria. Int. J. Climatol. 2017; 37(S1): 179-192.
48. Zohrevandi A. A., Sagheb Talebi K. Distribution pattern of Wild pear (Pyrus spp.) in the forests of Kermanshah Province of Iran. Appl. Biol. 2021; 33(4): 165-178.
49. Shahbazi Kh., Khosroshahi M., Heshmati M., Saieedifar Z. Effects of climate change on dust storm occurrence in Kermanshah Province, Iran. ECOPERSIA 2022; 10(2):121-131.
50. Zolfaghari H., Sahrai J., Sahaghobadi F., Jalilian A. Analysis on synoptic and dynamic aspects of air pollution in Kermanshah city. J.Geo.Environ. Hazard. 2014; 3(1):75-96.
51. Ghorbanian A., Mohammadzadeh A., Jamali S., Duan Z. Performance evaluation of six gridded precipitation products throughout Iran using ground observations over the last two decades (2000–2020). Remote Sens. 2022; 14(15): 3783.
52. Huffman G. J., Bolvin D. T., Braithwaite D., Hsu K., Joyce R., Xie P., Yoo S. H. NASA global precipitation measurement (GPM) integrated multi-satellite retrievals for GPM (IMERG). Algorithm Theoretical Basis Document (ATBD) Version, 2015; 4(26).
53. Tan J., Huffman G.J., Bolvin D.T., Nelkin E.J. IMERG V06: Changes to the morphing algorithm. J. Atmos. Ocean. Technol.2482–2471 :(12)36 ;2019 .
54. Koster R. D., Liu Q., Reichle R. H., Huffman G. J. Improved estimates of pentad precipitation through the merging of independent precipitation data sets. Water Resour. Res. 2021; 57(12): e2021WR030330.
55. Ali G., Sajjad M., Kanwal S., Xiao T., Khalid S., Shoaib F., Gul H.N. Spatial–temporal characterization of rainfall in Pakistan during the past half-century (1961–2020). Sci. Rep. 2021; 11(1):1-15.
56. Zhang G., Tian G., Cai D., Bai R., Tong J. Merging radar and rain gauge data by using spatial–temporal local weighted linear regression kriging for quantitative precipitation estimation. J. Hydrol. 2021; 601: 126612
57. Martínez-González A., Monzó-Cabrera J., Martínez-Sáez A.J., Lozano-Guerrero A.J. Minimization of measuring points for the electric field exposure map generation in indoor environments by means of Kriging interpolation and selective sampling. Environ. Res. 2022;212(Part D): 113577.
58. Oliver M.A., Webster R. A tutorial guide to geostatistics: Computing and modelling variograms and kriging. Catena 2014;113(1): 56-69.
59. Kambhammettu BVNP, Allena P., King J.P. Application and evaluation of universal kriging for optimal contouring of groundwater levels. J. Earth Syst. Sci. 2011; 120(3): 413-422.
60. Govaerts Y. M., Verstraete M. M. Raytran: A Monte Carlo ray-tracing model to compute light scattering in three-dimensional heterogeneous media. IEEE Tran. Geosci. Remote Sens., 1998; 36(2): 493-505
61. Milewski A., Elkadiri R., Durham M. Assessment and comparison of TMPA satellite precipitation products in varying climatic and topographic regimes in Morocco. Remote Sens. 2015; 7(5): 5697-5717.
62. Duan Z., Bastiaanssen W. G. M. Estimating water volume variations in lakes and reservoirs from four operational satellite altimetry databases and satellite imagery data. Remote Sens. Environ. 2013; 134(1): 403-416.
63. Darand M., Amanollahi J., Zandkarimi S. Evaluation of the performance of TRMM Multi-satellite Precipitation Analysis (TMPA) estimation over Iran. Atmos. Res. 2017; 190(1):121-127.
64. Pirmoradian R., Hashemi H., Fayne J. Performance evaluation of IMERG and TMPA daily precipitation products over CONUS (2000–2019). Atmos. Res. 2022; 279: 106389.
65. Haberlandt U. Geostatistical interpolation of hourly precipitation from rain gauges and radar for a large-scale extreme rainfall event. J. Hydrol. 2007; 332 (1-2):144–157.
66. Verworn A., Haberlandt U. Spatial interpolation of hourly rainfall–effect of additional information, variogram inference, and storm properties. Hydrol. Earth Syst. Sci. 2011; 15(2): 569-584.
67. Berndt C., Haberlandt U. Spatial interpolation of climate variables in Northern Germany—Influence of temporal resolution and network density.J. Hydrol. Reg. Stud. 2018; 15(C):184-202.
68. Zou W.Y., Yin S.Q., Wang W.T. Spatial interpolation of the extreme hourly precipitation at different return levels in the Haihe River basin. J. Hydrol.2021; 598(4):126273.
69. Wang Z., Zhong R., Lai C. Evaluation and hydrologic validation of TMPA satellite precipitation product downstream of the Pearl River Basin, China. Hydrol.Process.2017;31(23):4169–4182.
70. Wang Z., Zhong R., Lai C., Chen J. Evaluation of the GPM IMERG satellite base precipitation products and the hydrological utility. Atmos. Res. 2017; 196(1): 151–163.
71. Alsafadi K., Mohammed S., Mokhtar A., Sharaf M., He H. Fine-resolution precipitation mapping over Syria using local regression and spatial interpolation. Atmos. Res. 2021; 256(1):105524.
72. Zandi O., Zahraie B., Nasseri M., Behrangi A. Stacking machine learning models versus a local-

ly weighted linear model to generate high-resolution monthly precipitation over a topographically complex area. Atmos. Res. 2022; 272: 106159.
73. Daly C., Slater M.E., Roberti J.A., Laseter S.H., Swift Jr LW High-resolution precipitation mapping in a mountainous watershed: ground truth for evaluating uncertainty in a national precipitation dataset. Int. J. Climatol. 2017; 37(1):124-137.
74. Ranhao S., Baiping Z., Jing T. A multivariate regression model for predicting precipitation in the Daqing Mountains. Mountain Res. Develop. 2008; 28(3): 318-325.